44th AIAA Aerospace Sciences Meeting and Exhibit
9 - 12 January 2006, Reno, Nevada

AIAA 2006-470

New Satellite Drag Modeling Capabilities

Frank A. Marcos*
Air Force Research Laboratory, Hanscom AFB, MA 01731-3010

This paper reviews the operational impacts of satellite drag, the historical and current capabilities, and requirements to deal with evolving higher accuracy requirements. Modeling of satellite drag variations showed little improvement from the 1960's to the late 1990's. After three decades of essentially no quantitative progress, the problem is being vigorously and fruitfully attacked on several fronts. This century has already shown significant advances in measurements, models, solar and geomagnetic proxies and the application of data assimilation techniques to operational applications. While thermospheric measurements have been historically extremely sparse, new data sets are now available from intense ground-based radar tracking of satellite orbital decay and from satellite-borne accelerometers and remote sensors. These data provide global coverage over a wide range of thermospheric altitudes. Operational assimilative empirical models, utilizing the orbital drag data, have reduced model errors by almost a factor of two. Together with evolving new solar and geomagnetic inputs, the satellite-borne sensors support development of advanced operational assimilative first principles forecast models. We look forward to the time when satellite drag is no longer the largest error source in determining orbits of low altitude satellites.

I. Introduction

Aerodynamic drag continues to be the largest uncertainty in precision orbit determination for satellites operating below about 600 km. Drag errors impact many aerospace missions including satellite orbit location and prediction, collision avoidance warnings, reentry prediction, lifetime estimates and attitude dynamics. Errors in neutral density are the major source of drag errors. Orbital drag accelerations (a_D) for a satellite in the earth's atmosphere are related to neutral density (ρ) by:

$$a_D = - \tfrac{1}{2} (C_D A/M) \rho V^2 \qquad (1)$$

where C_D, A, M and V are respectively the satellite drag coefficient, cross-sectional area, mass, and velocity relative to the ambient gas. After density, the other terms in order of importance are (assuming A/M is known) generally the satellite's drag coefficient, C_D, and the neutral wind. The neutral wind enters the drag equation through the total atmospheric velocity relative to the satellite. A typical 200 m/sec winds contributes about 5% to the total drag. During large geomagnetic storms, winds of the order of 1 km/sec have been observed.

Thermospheric density is driven mainly by two solar influences: EUV radiation (solar photons) and the solar wind (corpuscular radiation). The solar EUV heating generally predominates, accounting on average for about 80% of the energy input to the thermosphere, and determines the basic thermospheric structure. Solar EUV variations exhibit a solar cycle, an approximately 27-day solar rotation period and day-to-day dependencies. Geomagnetic storms follow similar temporal trends but are more episodic. The thermosphere is thus a dynamic region mainly dependent on the relative heating due to the variable solar EUV radiation at low latitudes and the auroral processes, associated with the solar wind, at high latitudes. A persisting problem for modelers has been the lack of solar EUV and auroral heating (particles and electric fields) data. In the absence of the needed solar observational data, empirical models have historically used the F10.7 solar radio flux as a proxy for solar EUV heating and the 3-hourly kp index to represent the level of geomagnetic activity.

* Physicist, Space Vehicles Directorate, AFRL/VSBXT, 29 Randolph Road; AIAA Member

Since the early space age, sparse upper atmosphere measurements have been incorporated into relatively simple, but effective models driven by solar heating proxies. While these models brought significant understanding of the processes causing atmospheric variability, their inherent accuracies showed little quantitative improvement, giving rise to the term "15% barrier". We now are experiencing a "Golden Age of Satellite Drag" with new programs to routinely measure drag and density globally, to develop new solar and geomagnetic indices and empirical and physical models and to implement sophisticated assimilation techniques. These programs are directed toward dramatically reducing satellite drag errors and increasing forecast times to meet stringent present and evolving operational capabilities.

II. Satellite Drag Models

Two versions of empirical models have been used extensively used to represent neutral upper atmospheric variability. The Jacchia (e.g. Ref. 1) models, developed between 1964 and 1977, are based mainly on satellite drag data. The Mass Spectrometer and Incoherent Scatter (MSIS) models developed between 1977 and 2002 (e.g. Ref 2), utilized atmospheric composition data from instrumented satellites and temperatures from ground-based radars. The major variations in the thermosphere: diurnal, seasonal, semiannual, solar activity and geomagnetic activity were first incorporated into the Jacchia 1964 (J64) model. J64 laid the foundation for models still used today. Height profiles of the major constituents were calculated as a function of exospheric temperature assuming diffusive equilibrium and fixed boundary conditions initially at 120 km. An exponential form for the temperature profile that was closely approximated by theoretical temperature profiles allowed the hydrostatic equation to be explicitly integrated to provide density as a function of altitude. The MSIS 77 model was based on the Jacchia temperature profile framework, but the density at 120 km varied with local time and other geophysical parameters to fit the measurements. Exospheric temperature and the density variation were represented by spherical harmonics resulting in requiring fewer parameters for a given level of accuracy.

Both types of models were updated over time. The new NRLMSISE-00 model[3] of atmospheric composition, temperature, and total mass includes the following data: (1) drag data based on orbit determination, (2) more recent accelerometer data sets, (3) new temperature data derived from Millstone Hill and Arecibo incoherent scatter radar observations, and (4) observations of $[O_2]$ by the Solar Maximum Mission (SMM), based on solar ultraviolet occultation. A new species, "anomalous oxygen," primarily for drag estimation, allows for appreciable O^+ and hot atomic oxygen contributions to the total mass density at high altitudes.

Figure 1 reviews the problem that confronted the scientific and operational users of neutral density models. One-sigma standard deviations[4] are given for models produced between 1964 and 1990. These evaluations showed that both types of models actually do remarkably well in describing the thermospheric variability. However, they all had similar one-sigma errors of about 15%. A notional depiction of the amount of data available for development of the various models is given as a solid line. New data sets yielded significant advances in understanding the morphology of drag variations but did not result in commensurate quantitative modeling improvements. For example the earliest Jacchia model used 10,000 orbital decay density values. This amount was increased to 40,000 points in the J77[5] model. The MSIS model was recognized as providing a superior description of the atmospheric composition. However, the Jacchia 1970[6] (J70) model is used operationally by a number of organizations including AF Space Command and NASA MSFC since it was available before the advent of the MSIS models, used less computer time and was equivalent in satellite drag accuracy.

The concept of successfully correcting neutral density models in near real time with satellite drag data[7] obtained from ground-based tracking data was demonstrated in 1998. A Special Perturbations orbit determination process best fits the tracking observations of "calibration" satellites (known area-to-mass ratio) in a least squares sense. This procedure solves for a ballistic coefficient (CdA/M) assuming the density was that predicted by the Jacchia 1970 model (see eq. 1) to best fit the observations. If the model density is low, then the ballistic coefficient is correspondingly increased. Conversely, if the model prediction is high, then the ballistic coefficient is lowered accordingly. Since the satellite's area-to-mass ratio was known, corrections to the ballistic coefficient are identical to corrections in model densities over the fit span (typically a few days). With these corrections applied to the model, measurements from a single calibration satellite were shown to be conceptually capable of globally reducing density model errors to the 5% level.

The data assimilation approach was optimized in the Air Force High Accuracy Satellite Drag Model (HASDM). The technique was been fully described at the AIAA Astrodynamics Specialists Conference in 2002[8,9]. Density

correction parameters are determined by simultaneously processing the satellite tracking observations from about 75 calibration satellites. The corrections are determined in a single weighted Special Perturbations differential correction across all the calibration satellites using their observations and statistical uncertainties directly while simultaneously solving for their states. This process can generate an average global density correction to J70 every three hours. The density corrections take the form of spherical harmonic expansions of two Jacchia temperature parameters that enhance spatial resolution. The concept was funded by the AF Space Battle Lab and tested in 2001. Operational testing was held in the summer of 2002 and operational implementation began in Sept 2004. HASDM currently typically reduces satellite drag errors from about 15% to 8% and provides a one-day forecast capability[10]. Thus the persisting deficiency in satellite drag operations has now been cut by about a factor of two in an operational setting.

A new HASDM 2 initiative[11] has a goal of a three-day forecast capability, increased accuracy, and extension to below 200 km. These objectives are being supported by tracking about 300 satellites. A major improvement in the J70 model parameters will be incorporation of an improved semiannual variation dependent on solar flux[12]. The current model relies on a climatological average value. Latitude and local time variations will also be upgraded from analysis of an extensive orbital drag database from 38 satellites covering the period 1979-2003. Completion of HASDM 2 development is planned for early 2006. Operational implementation is anticipated in 2008.

HASDM 2 will also emphasize sue of new solar proxy tools. The 10.7 cm proxy is from coronal radio emissions, but some of the strongest lines in the EUV spectrum are emitted from the solar chromosphere. The new E10 index[13], tested as part of the first HASDM program, derived full spectrum EUV with the F10 index driving coronal lines and the Mg index driving chromospheric lines. Recently, new indices representing major improvements in specifying the solar EUV and UV inputs have been reported[14]. It has been shown that the far ultraviolet (FUV) energy in the Schumann-Runge Continuum , absorbed at lower altitudes, near 120 km, also contributes to density variability with a lag of about 5 days. Therefore a new Esrc index was developed to further reduce density uncertainties and to improve forecasts. Updated background solar EUV radiances E10.7 and XE10.7 are calibrated to the TIMED/SEE data. The TIMED Solar EUV Experiment (SEE) directly measures the soft x-ray (XUV) from 0 to 30 nm and the far ultraviolet (FUV) from 120 to 200 nm as well as the extreme ultraviolet (EUV) from 0 to 120 nm. XE10.7 represents the integrated 1-40 nm bandpass energy and has a slightly better correlation with density variability than the E10.7 index which is integrated over the full spectrum. Finally, flares above the background irradiance also contribute to atmospheric heating. High-time resolution solar x-ray flare evolution indices are being developed. These indices will all be tested as part of the HASDM 2 upgrade.

An improved proxy to replace the geomagnetic activity index Kp is being developed based on the Joule power[15]. The Joule power, closely associated with the level of geomagnetic heating, is better parameterized using the PC index and the Dst index. PC (Polar Cap index) is a ground based measurement of the strength and orientation of the ionospheric current in the polar cap. Dst (Disturbance Storm Time index) is measured by low latitude magnetometers. This index will also be tested as part of HASDM 2.

One of the outstanding challenges in thermospheric forecasting continues to be capturing the thermospheric response to periods of intense energy input during geomagnetic storms. A physical model, e.g. CTIM[16] (Coupled Thermosphere-Ionosphere Model) is needed since empirical models lack a capability to follow the dynamic density changes during geomagnetic storms. Current physical models are statistically about as accurate as empirical models. Further, they can reproduce generic geomagnetic storm effects. Modeling specific storms is still a challenge because currently, available observational capability does not permit adequate knowledge of the spatial and temporal distribution of storm inputs. This shortcoming is being addressed by using measurements of the thermospheric response and removing errors using data assimilation techniques. The success of tropospheric weather forecasts has been due to (1) improvements in capturing physical processes in the numerical models, (2) very dense measurements and (3) capability to combine the two with optimal data assimilation techniques. For the thermosphere-ionosphere system, the first condition is currently being addressed. In addition to current processes incorporated into physical models, new heating sources effective during very large storms and not detectable by ground-based magnetometers have recently been discovered[17]. Dense measurements are forthcoming as described in the section below. Optimal data assimilation techniques are under development[18]. Thus the future AF goal of a more accurate assimilative coupled thermosphere-ionosphere forecast model is now realizable.

III. New Measurements

Thermospheric density measurements were historically sparse in the previous century. New measurements are providing a rich abundance of data vs altitude, latitude, local time day of year and solar and geomagnetic conditions. As an example of the explosion in neutral density data availability, Figure 2 compares thermospheric measurements in the 1980-1999 20-year period vs the new data sets that have become available in the first five years of this century. The data sources[10] include the CHAMP (CHAllenging Minisatellite Payload) and GRACE (GRAvity and Climate Experiment) accelerometers, the TIMED (Thermosphere Ionosphere Mesosphere Energetics and Dynamics) GUVI (Global UltraViolet Imager) and operational DMSP SSULI (Special Sensor Ultraviolet Imager) and SSUSI (Special Sensor Ultraviolet Spectrographic Imager) density remote sensors and rejuvenated long-term orbital drag measurements.

AFRL has analyzed orbital drag, accelerometer and remote sensing data as part of a DMSP SSUSI neutral density remote sensing cal-val effort. Samples of these data are presented to illustrate new aspects of density variations vs latitude, local time, solar flux and geomagnetic activity.

A. Orbital Drag Measurements

Orbital decay measurements provided the first realistic upper atmosphere measurements. They are the basis for the J70 model still utilized operationally at Air Force Space Command and NASA. This measurement technique was recently exploited and greatly improved to develop a comprehensive, high-resolution historical database needed to permit evaluation and improvement of empirical models. The database achieved one-day resolution[19] for the first time and provided unprecedented coverage in solar/geographic conditions. The data are estimated to be accurate to within about +/- 4%. We refer to this data set, funded by the NASA LWS (Living With a Star) program as the AFRL/LWS database. Figure 3a summarizes the database in altitude-time coordinates. Data obtained by 26 satellites cover the time period 1966-2003 and the altitude region 235-600 km. The spatial resolution is described in Figure 3b. This figure shows the fractional drag for a polar orbit with perigee at the equator. For a 350 x 3000 km orbit, 90% of the drag occurs between +/- 20 degrees of perigee. Figure 3c shows thermospheric density variability and model ratios at 400 km altitude vs solar and geomagnetic activity over a thirty-year period. The density can vary by more than an order of magnitude over a solar cycle, but model ratios are generally within 20% of unity. Results for this database permitted descriptions of accuracies for the J70, NRLMSISE-00 and NASA MET[20] models vs all the relevant parameters and specifically identified deficiencies in empirical model Fbar and F-Fbar terms. AFRL plans to expand its database beyond 2004. Historic databases are also being generated by AFSPC[12] and NRL[21]. Therefore a vast and growing repository of neutral density data will continue to be available over a wide range of latitude and local time conditions from the 1960's into the future.

An unexpected result has been the detection of long-term unmodeled thermospheric variations[22]. First principle model simulations[23] had predicted that a doubling of CO_2 , expected in the mid-21st century, would cause thermospheric density to decrease by about 40% at 400 km at solar minimum conditions and 18% at solar maximum. Figure 3d shows ratios of data from five satellites near 400 km to the J70 model from 1970 – 2000. The normalized data were obtained by removing the model error in Fbar. These data indicate a density decline of about 5% over 30 years (average solar flux of 128 units) corresponding to a CO_2 increase of 12.5%. The consequence is longer satellite lifetimes for space objects. Lewis et al[24] provided the first investigation of thermospheric cooling effects upon the space debris population. Their scenario was based on a model of debris evolution over a one hundred year period. It showed that a combination of increased lifetimes and, mainly, increased number of collisions led to a predicted increase of average number of objects >1cm and >10 cm by about 30% and 10% respectively, due solely to thermospheric cooling. Such studies, while speculative, illustrate the continuing applications and requirements for improved satellite drag models over all time scales.

B. Satellite Accelerometer Measurements

Accelerometers aboard CHAMP and GRACE continue to provide unprecedented new high-resolution neutral density data. Figure 4 shows the spacecraft (CHAMP top left, GRACE bottom left), the STAR (Spatial Triaxial Accelerometer for Research) accelerometer[25] (top right), and typical data (bottom left) from one orbit of CHAMP. The CHAMP satellite was launched 15 July 2000 into a near circular, near polar (i = 87°) orbit with an initial altitude of about 450 km. The 5-year design lifetime of CHAMP has been exceeded. The satellite is sampling

increasingly lower altitudes (currently near 370 km) and is expected to continue to lower altitudes through solar minimum and beyond. The GRACE mission, launched 17 March 2002 into an 89-degree inclination orbit with an initial perigee near 500 km, uses a more sensitive version of STAR (SuperSTAR) on each of two satellites separated by a nominal 220 km. The data reduction procedures used for CHAMP, and generally adopted in the current GRACE analysis have been described by Bruinsma et al[25].

Figure 5 (top) shows CHAMP density data for July-Sept 2002 acquired for our cal val effort. Data, plotted in latitude vs day of year coordinates, are normalized to 350 km using the NRLMSISE-00 model to remove variations due to altitude. Results are shown as one-day averages (centered at 0 UT) and are based on daytime data only. Corresponding ratios of CHAMP densities to NRLMSISE-00 model predictions are shown in the middle chart, and solar-geomagnetic activity at the bottom. The data are for quiet and moderately disturbed geomagnetic activity and moderate to high solar flux. The CHAMP orbit shifts from 13/01 LT to 9/21 LT from 3 July to 30 September 2002. This data sample reveals several density features not well represented by current thermospheric models: (a) The time period up to about 10 Aug (day 222) shows densities that are significantly lower than in succeeding days. The model overestimation of the density by over 20% is attributed to anomalous solar flux variations not captured by the model's F10 solar proxy. The Solar EUV Experiment (SEE) on the TIMED satellite shows a corresponding decrease in the FE XV 28.4 nm coronal emission[26]. The period dominated by chromospheric lines is associated with lower thermospheric densities. Therefore, the F10 index, representative of coronal emissions, is a particularly unreliable proxy during this period. Assimilation techniques can correct the specification of density. However, even a very accurate forecast of F10 would lead to unacceptable satellite drag prediction errors. This anomaly further emphasizes the need for more realistic solar proxies.

Extreme thermospheric variability is illustrated by data from the superstorm of 8-10 Nov 2004. GRACE response is shown in Figure 6a, with corresponding model response in Figure 6b. Geomagnetic activity maximized during days 312 – 315, with ap reaching 300 on two consecutive 3-hr intervals on day 313 and again at the end of day 314 and middle of day 315. To facilitate interpretation of the variability, densities in 2-degree latitude bins were normalized to the quiet conditions of day 311. Altitudes in each bin only vary by a few km over the time period studied so any error due to altitude variation is very small compared to the large storm-induced variations. Since a detailed description of this storm is beyond the scope of this paper, only highlights of the complex response are given here.

The variations are very large, reaching values of over a factor of 5.The full latitudinal coverage reveals that the winter hemisphere response is greater than that in the summer. The nightside response is generally higher than that of the dayside. Density ratios at the dayside equator during the first half of day 313 are about a factor of 2.5 while those on the nightside are greater than 3 and reach a factor of 6.6 at 5.2 hr UT. The data also indicate a more efficient propagation of the disturbance into lower latitudes on the nightside, consistent with theoretical predictions[16]. Corresponding ratios of measured density to NRLMSISE-00 (Figure 6b) show that the model underestimates the storm response by as much as a factor of three. These findings further emphasize the need for realistic first principles models that can capture the dynamic response of the thermosphere to geomagnetic disturbances.

C. Remote Sensing Measurements

The Defense Meteorological Satellite Program (DMSP) F16 spacecraft, launched Oct 2003, carried two operational neutral upper atmospheric (and ionospheric) remote sensing instruments. SSUSI[27] and SSULI[28] These instruments are designed to provide near real time data as input into models of the thermosphere and ionosphere.. Four additional SSUSI and SSULI have been built for flights on forthcoming DMSP satellites, ensuring a long-term monitoring capability.

SSULI is designed to view Earth's limb and measure vertical profiles of thermospheric composition from appropriate airglow emissions at tangent altitudes of approximately 50 km to 750 km. A SSULI prototype has been flown, as noted in Figure 2. The LORAAS (Low-Resolution Airglow and Auroral Spectrograph), was launched in Feb 1999 on the ARGOS (Advanced Research and Global Observation Satellite). A potential for deriving neutral density from this limb-scanning technique[29] was demonstrated during this flight. However, the remainder of this section relates to validating data from GUVI (Global UltraViolet Imager)[29], which is based on SSUSI heritage.

GUVI is a far-ultraviolet (115 to 180 nm), scanning imaging spectrograph that provides horizon-to-horizon images in five selectable wavelength intervals, or "colors" that are due to the major constituents, N_2, O_2, O, and H, of the upper atmosphere. It measures the composition and temperature profile of the upper atmosphere (as well as its auroral energy inputs). GUVI is the first instrument sensitive enough to look, in detail, at composition changes in the upper atmosphere.

The major functional elements of GUVI, shown in Figure 7a, are: a scanning imaging spectrograph (SIS) that obtains the spectral data, a detector processor which converts information recorded at the detector into wavelength and spatial information as required, and an interface to the spacecraft. GUVI uses a scan mirror to sweep its 11.78 degree field-of-view through an arc of up to 140 degrees in the plane perpendicular to the orbital plane. The scan is from horizon-to-horizon and up to a 520-km tangent altitude onto the limb that is away from the Sun (see Figure 7b). This instantaneous field-of-view is mapped via the spectrograph into 14 spatial and 160 spectral "pixels". A detector processor bins the data into the five selected colors.

GUVI was launched on the TIMED satellite on 7 Dec 2001 into a circular 630 km, 74-degree inclination orbit. Neutral density measurements are obtained during daytime conditions and for latitudes below the auroral zone. Approximately 33 altitude profiles are obtained each orbit. Data are obtained at a tangent height and therefore over a line-of-sight typically of order of 2500 km. A sample of GUVI neutral densities, obtained by summing over the atmospheric constituents, is given vs latitude and time in Figure 7c. Data shown are one-day averages and are normalized to an altitude of 350 km. Measurements generally cover the altitude region +/- 60 degrees. Gaps indicate periods where the solar zenith angle exceeds 80 degrees and the data reduction algorithm is not applicable. As was observed with the accelerometer data, the GUVI measured densities are lower during July than in September. This data sample is indicative of the comprehensive thermospheric composition, temperature and density data available from early 2002 to the present[30]. The GUVI data are compared to GRACE densities in Figure 7d. To account for differences in latitude and local time of the two data sets, both GUVI and GRACE data are plotted as ratio to the respective values of NRLMSIS. Therefore the parameter plotted is the ratio of GRACE to model divided by the ratio of GUVI to model. The two data sets are in very good agreement. There is an offset between the absolute densities. GRACE shows more high latitude response to the geomagnetic storm on day 250, although this may be due to the model capability to capture the storm response at the different local times of the two datasets.

A comparison of orbital drag, the normalized accelerometer data and GUVI remote sensing is given in Figure 8. All data are one day averages, centered on 0 UT, are for the 0-30 degree latitude bin, are normalized to 350 km and are shown as ratio to NRLMSISE-00 to mainly minimize local time differences. The agreement between the drag measurements and remote sensing is excellent. On average the GUVI data agree with the AFRL/LWS data to within the accuracy of the drag data. This is believed to be the first comparison of these techniques. The result demonstrates the fidelity of the GUVI data, as well as its value in data assimilation schemes using first principles models. A further analysis reveals slight latitudinal differences between the accelerometer and GUVI data. Figure 9 shows data obtained in 3-hour intervals as a function of latitude (5-degree resolution) and time for July-Sept 2002. Both CHAMP and GUVI are compared as ratio to MSIS. This permits comparing data normalized to the same altitude and at the same latitude bins and Universal time bins with the model accounting mainly for local time differences. The quantity compared is (CHAMP/MSIS)/(GUVI/MSIS). This ratio decreases from 0.97 at the equator to0.88 at 30 degrees then increases to about 0.89 at 55 degrees. Further analysis is required to confirm that the accelerometer data provide the correct latitudinal dependence. However, a trend for higher accelerometer densities than predicted by models has been examined and supported in recent studies.

IV. Discussion and Summary

Uncertainties in neutral density variations have been the major limiting factor for precision low earth orbit determination. The combined vast new data sets from orbital drag, satellite-borne accelerometers and remote sensors provide unprecedented capabilities to understand thermospheric variability. Solar EUV heating is the major energy source for the thermosphere and is also the major source of day-to-day satellite drag errors. Data are revealing new areas of thermospheric sensitivity to solar EUV. These issues can now be addressed with new, accurate measurements of the solar spectrum. The dramatic, though less frequent, geomagnetic storm effects can now be analyzed with detail previously unavailable. Variations vs latitude, day of year and local time are being defined with high resolution. After three decades of essentially no quantitative progress, the satellite drag problem is

being vigorously and fruitfully attacked on several fronts: a variety of comprehensive measurements, data assimilation or "calibration" schemes, solar and geomagnetic indices, and numerous relevant space weather studies.

Acknowledgments

Data analysis support to AFRL was provided by Boston College. Brian Sullivan, P.I. was expertly supported by Carolyn Parsons and Don Mizuno. J. O. Wise, AFRL, lent in-house support. Much of this paper used unpublished data provided to us by various mechanisms. R. R. Meier, GMU, contributed his upgraded GUVI data and technical expertise. GRACE data processing at CSR, Univ. of Texas at Austin was under Byron Tapley, supported by P.A.M. Abusali, M. K. Cheng, J. Ries and S. Bettadpur. CHAMP data processing at Univ. of Colorado was under S. Nerem and Jeff Forbes, with the support of E. Sutton. B. R. Bowman, AFSPC, provided additional orbital drag data and technical discussions. J. M. Picone, NRL offered continuing valuable suggestions and advice on data comparison methodology. Larry Paxton, JHU/APL, guided the direction of technical studies. Paul Straus, Aerospace Corp coordinated the overall cal val effort.

References

[1]Jacchia, L, G., Static Diffusion Models of the Upper Atmosphere with Empirical Temperature Profiles, SAO Special Report No. 170, 1964.

[2]Hedin, A. E., Reber, C. A., Newton, G. P., Spencer, N. W., Brinton, H. C., Mayr, H. G., and Potter, W. E., A global thermospheric model based on mass spectrometer and incoherent scatter data: MSIS 2 composition, J. Geophys. Res., 82, 2148, 1977.

[3]Picone, J. M., A. E. Hedin, D. P. Drob, and A. C. Aiken, NRLMSISE-00 empirical model of the atmosphere: Statistical comparisons and scientific issues, J. Geophys. Res., 107, 1468, 2002.

[4]Marcos, F.A., Accuracy of atmospheric drag models at low satellite altitudes, Adv. Space Res., 10, 417, 1990.

[5]Jacchia, L. G., Thermospheric Temperature, Density, and Composition: New Models, SAO Special Report No. 375, 1977.

[6]Jacchia, L. G., Revised static models of the thermosphere and exosphere with empirical temperature profiles, SAO Special Report No. 313, 1970.

[7]Marcos, F.A., M. Kendra, J. Griffin, J. Bass, J. Liu and D. Larson, Precision low earth orbit determination using atmospheric density calibration, Jnl Astron. Sci., 46, 395, 1998.

[8]Storz, M.F., B.R. Bowman and Branson, J.I. (Maj), High Accuracy Satellite Drag Model (HASDM), AAS/AIAA Astrodynamics Specialist Conference, paper AIAA 2002-4886, Monterey, CA, 2002.

[9]Casali, S. J. W. N. Barker and M. F. Storz, Dynamic Calibration Atmosphere (DCA) Tool for the High Accuracy Satellite Drag Model (HASDM), AAS/AIAA Astrodynamics Specialist Conference, paper AIAA 2002-4888, Monterey, CA, 2002.

[10]Marcos, F. A., New Measurements of Thermospheric Density: A Review, AAS/AIAA Astrodynamics Specialist Conference, paper AIAA 05-251, Lake Tahoe, CA, 2005.

[11]Bowman, Bruce R., HASDM, Sapphire Dragon Projects, presented at Atmospheric Neutral Density and Solar Indices Workshop, AFSPC, Colorado Springs, CO, 12 Oct 2005.

[12]Bowman, B. R, The semiannual thermospheric density variation from 1970 to 2002 between 200-1100 km, AAS-04-173, AAS/AIAA Fight Mechanics Meeting, Maui, HI, 2004.

[13]Tobiska, W. K., Validating the solar EUV proxy, $E_{10.7}$, J. Geophys. Res., 106, 29969-29978, doi: 10.1029/2000JA000210, 2001.

[14]Tobiska, W. K. and S. D. Bouwer, New Developments in SOLAR 2000 for Space Research and Operations, Adv. Space Res., in press, 2005.

[15]Knipp, D., W. K. Tobiska and B. A. Emery, Direct and Indirect Thermospheric Heating Sources for Solar Cycles 21–23, Solar Physics, 224 doi: 10.1007/s11207-005-6393-4, 2004.

[16]Fuller-Rowell, T.J., M. V. Codescru and R.J. Moffett, Response of the thermosphere and ionosphere to geomagnetic storms, J. Geophys. Res, 99, 3893-3914, 1994.

[17]Huang C. Y., W. J. Burke, Transient sheets of field-aligned current observed by DMSP during the main phase of a magnetic superstorm, J. Geophys. Res., 109, doi:10.1029/2003JA010067, 2004.

[18]Fuller-Rowell, T. J., C.F. Minter and M.V. Codrescu, Data assimilation for neutral thermospheric species during geomagnetic storms, Radio Sci., 39, doi:10.1029/2002RS002835, 2004.

[19]Bowman, B. R., F. A. Marcos, and M. J. Kendra, A method for computing accurate daily atmospheric density values from satellite drag data, AAS-04-173, AAS/AIAA Flight Mechanics. Mtg, Maui, HI, 2004.

[20]Owens, J.K., NASA Marshall Engineering Thermosphere Model - Version 2.0 , NASA/TM-211786, George C. Marshall Space Flight Center Marshall Space Flight Center, AL 35812, National Aeronautics and Space Administration Washington, DC 20546-0001, June 2002.

[21]Picone J. M., J. T. Emmert, J. L. Lean, Thermospheric densities derived from spacecraft orbits: Accurate processing of two-line element sets, J. Geophys. Res., 110, A03301, doi:10.1029/2004JA010585, 2005.

[22]Marcos, F. A. J. O. Wise, M. J. Kendra, N. J. Grossbard and B. R. Bowman, Detection of a long-term decrease in thermospheric neutral density, Geophys. Res. Lett.,32, doi: 10.1029/ 2004GL021269, 2005.
[23]Roble, R. G. and R. E. Dickinson, How will changes in carbon dioxide and methane modify the mean structure of the mesosphere and thermosphere?, Geophys. Res. Lett., 16, 1441-1144, 1989.
[24]Lewis, H. G., G. G, Swinerd, C. S. Ellis and C. E. Martin, Response of the space debris environment to greenhouse cooling, Fourth European Conference on Space Debris, Darmstadt, Germany, 18-20 April, 2005.
[25]Bruinsma, S., D. Tamagnan and R. Biancale, Atmospheric densities derived from CHAMP/STAR accelerometer observations, Plan. Spa. Sci., 52, 297-312, 2004.
[26]Woods, T.N., F. G. Esparvier, S. M. Bailey, P. C. Chamberlin. J. Lean, G. J. Rottman, S. C. Solomon, W. K. Tobiska and D, L, Woodraska, Solar EUV Experiment (SEE): Mission overview and first results, J. Geophys. Res., 110, AO1312, doi:1029/ 2004JA010765, 2005.
[27]Paxton, L. J. et al., Special Sensor UV Spectrographic Imager (SSUSI): An instrument description, Instrum. Planet. Terr. Atmos. Remote Sens.,1745, 2-16, 1992.
[28]Meier, R. R., J. M. Picone, Retrieval of absolute thermospheric concentrations from the far UV dayglow: An application of discrete inverse theory, J. Geophys. Res., 99, 6307-6320, doi:10.1029/93JA02775, 1994.
[29]Nicholas, A.C., S.E. Thonnard, K.F. Dymond, S. A. Budzien, S.H. Knowles, E.E. Henderlight and R. P. McCoy, Comparison of Ultraviolet Airglow Derived density to satellite drag derived density, AIAA 2002-4735, AAS/AIAA Astrodynamics Specialist Conference, Monterey, CA, 2002.
[30]Christensen, A. B. et al., Initial observations with the Global Ultraviolet Imager (GUVI) in the NASA TIMED satellite mission, J. Geophys. Res, 108, 1451, do1:10,1029/2003JA009918, 2003.

Figures

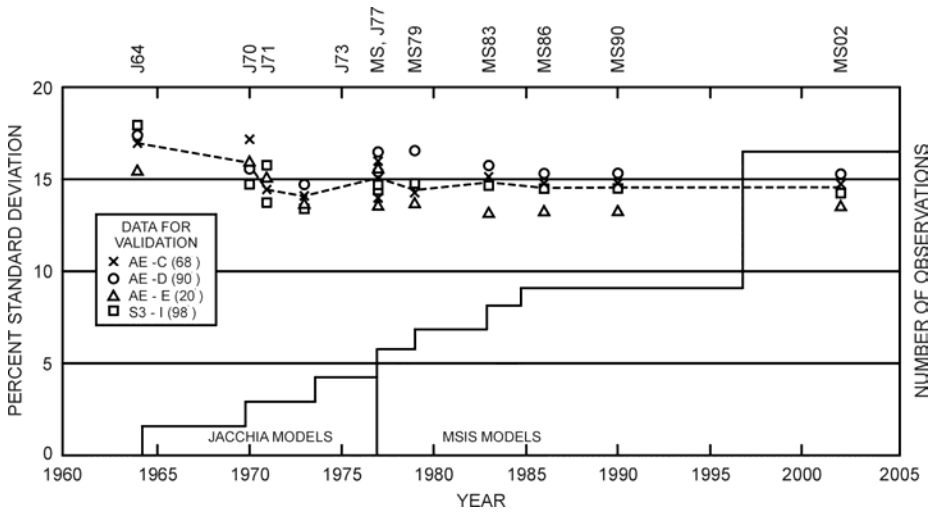

Figure 1 Empirical neutral density model accuracies vs time

Year	Experiment	Data	Lifetime	Agency
1981	DE-2	Composition	18 Mos.	NASA
1982	SETA-2	Density	8 Mos.	AFRL
1983	SETA-3	Density	8 Mos.	AFRL
1985	S85-1	Density	3 Mos.	AFRL
1988	San Marco	Density	8 Mos.	NASA
1999	LORAAS	Composition	3 Yrs.	NRL
2000	CHAMP	Density	5+ Yrs.	GFZ Potsdam
2001	TIMED GUVI	Composition	4+ Yrs.	NASA/APL/Aerospace
2002	GRACE	Density	3+ Yrs.	CSR, Texas
2003	SSULI/SSUSI	Composition	3+ Yrs.	DMSP/APL/NRL
2003	ORBITAL DRAG	Density	30+ Yrs.	AFRL/AFSPC/NRL

Figure 2 Satellite density measurements before and after the year 2000

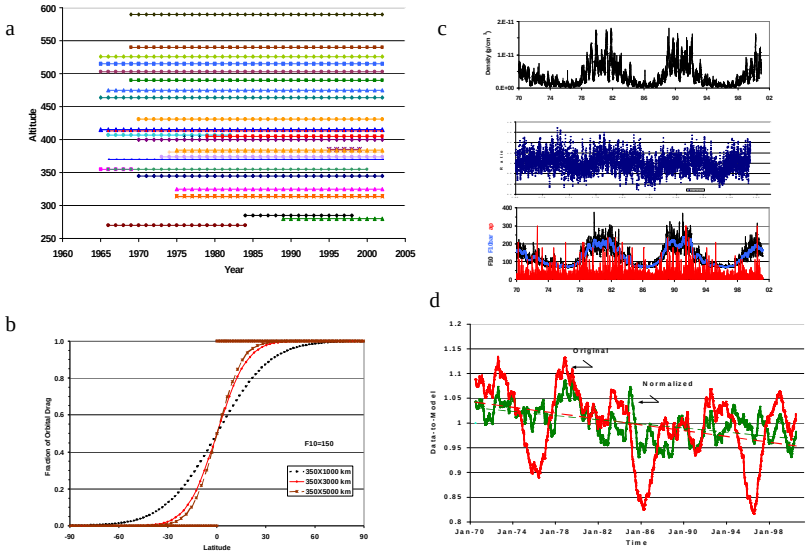

Figure 3 AFRL/LWS orbital drag database: (a) Data in altitude-day of year coordinates, (b) example of spatial resolution, (c) density at 400 km, data to model ratio and solar geomagnetic conditions, (d) model ratios showing downward trend with time.

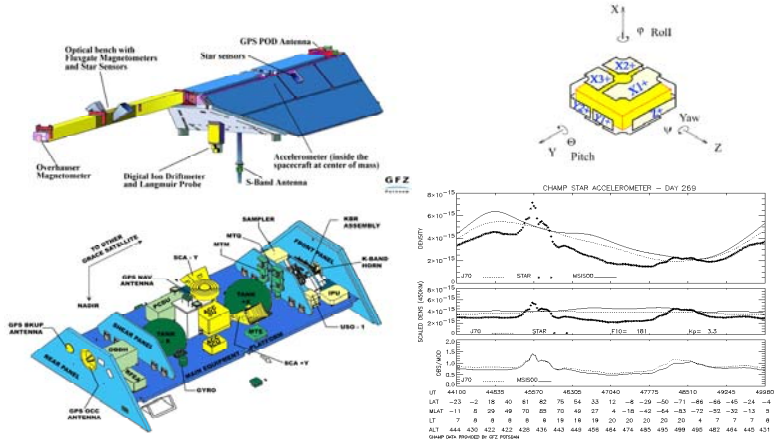

Figure 4 CHAMP & GRACE spacecraft configurations (left, top and bottom respectively) accelerometer package (top right) and data sample (bottom right).

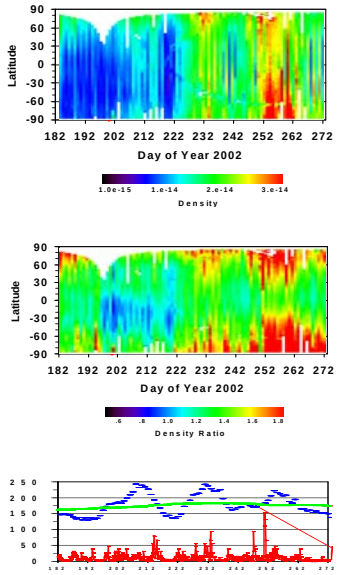

Figure 5: Top: GRACE accelerometer data in latitude-day of year coordinates for July-Sept 02 period; Middle: Ratio of data to NRLMSISE-00 model; Bottom: Solar-geomagnetic conditions.

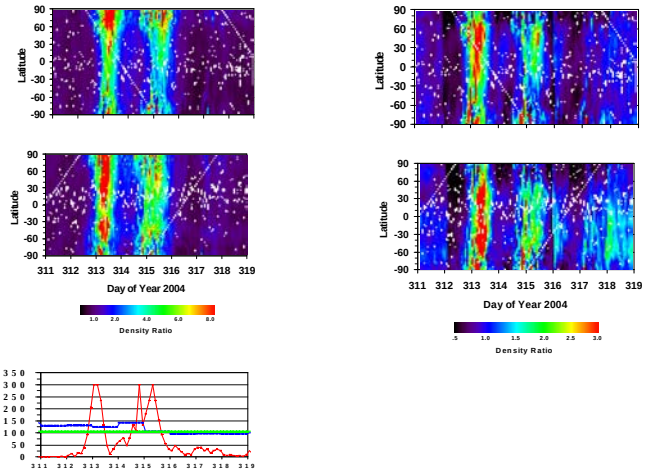

Figure 6 GRACE data for Nov 04 Geomagnetic Storm (See text).

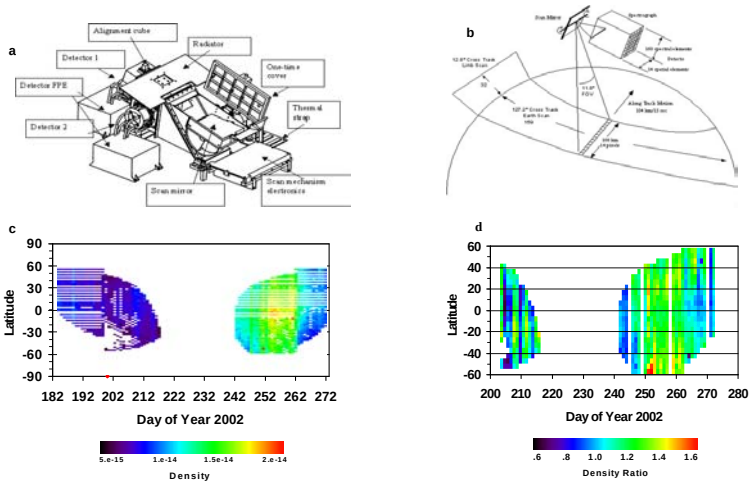

Figure 7 (a) GUVI major systems, (b) GUVI scanning capability, (c) sample GUVI data vs latitude, normalized to 350 km, for July-Sept 2002 period, (d) Ratio vs latitude of GUVI to model vs GRACE to model.

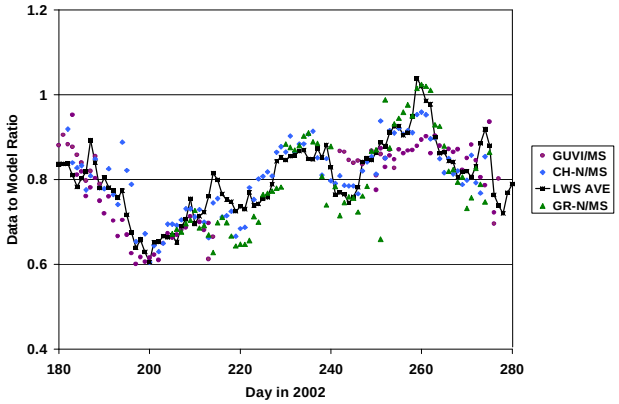

Figure 8 Normalized CHAMP and GRACE densities, AFRL orbital drag data and GUVI remote sensing data, all as ratio to NRLMSISE-00. All data are daily averages in the 0 +/- 30 degree latitude region.

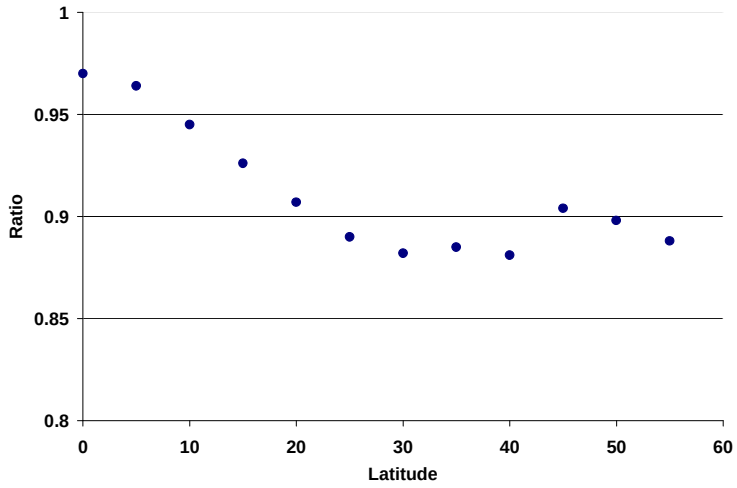

Figure 9 Average Ratio of GUVI/CHAMP vs Latitude for Period July-Sept 2002.